HHS Public Access

Author manuscript

Eur Respir J. Author manuscript; available in PMC 2018 April 24.

Published in final edited form as:

Eur Respir J. 2017 September ; 50(3): . doi:10.1183/13993003.00345-2017.

Predicting epiglottic collapse in patients with obstructive sleep apnea

Ali Azarbarzin, PhD[1], **Melania Marques, MD**[1,2], **Scott A Sands, PhD**[1,3], **Sara Op de Beeck, MSc**[4], **Pedro R. Genta, MD**[2], **Luigi Taranto-Montemurro, MD**[1], **Camila M de Melo, MSc**[1,6], **Ludovico Messineo, MD**[1], **Olivier M. Vanderveken, MD, PhD**[4,5], **David P White, MD**[1], and **Andrew Wellman, MD, PhD**[1]

[1]Division of Sleep and Circadian Disorders, Brigham and Women's Hospital and Harvard Medical School, Boston, Massachusetts

[2]Pulmonary Division, Heart Institute (InCor), Hospital das Clínicas, University of São Paulo School of Medicine, São Paulo, Brazil

[3]Department of Allergy Immunology and Respiratory Medicine and Central Clinical School, The Alfred and Monash University, Melbourne, Australia

[4]Translational Neurosciences, Faculty of Medicine and Health Sciences, University of Antwerp, Antwerp, Belgium

[5]Department of ENT, Head and Neck Surgery, Antwerp University Hospital, Edegem, Belgium

[6]Department of Psychobiology, Federal University of São Paulo, Brazil

Abstract

Objectives—Obstructive sleep apnea (OSA) is characterized by pharyngeal obstruction occurring at different sites. Endoscopic studies reveal that epiglottic collapse renders patients at higher risk of failed oral appliance therapy or accentuated collapse on CPAP. Diagnosing epiglottic collapse currently requires invasive studies (imaging, endoscopy). Alternatively, we propose that epiglottic collapse can be detected from distinct airflow patterns it produces during sleep.

Methods—Twenty-three OSA patients underwent natural sleep endoscopy. A total of 1232 breaths were scored as epiglottic/non-epiglottic collapse. Several flow characteristics were determined from the flow signal (recorded simultaneously with endoscopy) and used to build a predictive model to distinguish epiglottic from non-epiglottic collapse. Additionally, ten OSA patients were studied to validate the pneumotachograph flow features using nasal pressure signals.

Corresponding Author: Ali Azarbarzin, Sleep Disordered Breathing Lab, 221 Longwood Avenue, Boston, MA 02115, Tel: 617 732 8456, Fax: 617 732 7337, aazarbarzin@bwh.harvard.edu.

Potential conflicts of interest: Drs. Azarbarzin, Marques, Genta, Op de Beek, and Messineo declare no conflicts of interest. Dr. Taranto-Montemurro serves as a consultant for Novion Pharmaceuticals Inc and Cambridge Sound Management. Dr. Sands serves as a consultant for Cambridge Sound Management. Dr. Vanderveken receives research support from SomnoMed Ltd., Inspire Medical Systems Inc., Nyxoah and ReVent, and he serves as a consultant for Nyxoah and Philips Electronics B.V.; Dr. White receives salary from Apnicure Inc and serves as a consultant for Philips Respironics and Night Balance. Dr. Wellman receives research support from Philips Respironics, Varnum Sleep Solutions, and Cambridge Sound Management, and he serves as a medical advisor to Bayer and Varnum.

Results—Epiglottic collapse was characterized by a rapid fall(s) in the inspiratory flow, more variable inspiratory and expiratory flow, and reduced tidal volume. The cross-validated accuracy was 84%. Predictive features obtained from pneumotachograph flow and nasal pressure were strongly correlated.

Conclusions—This study demonstrates that epiglottic collapse can be identified from the airflow signal measured during a sleep study. This method may enable clinicians to use clinically-collected data to characterize underlying physiology and improve treatment decisions.

INTRODUCTION

Obstructive sleep apnea (OSA) is a common disorder characterized by recurrent upper airway collapse during sleep[1], which causes sleep fragmentation[2] and sympathetic activation[3]. A number of drug-induced sleep endoscopy (DISE) studies in OSA patients have demonstrated that the upper airway obstruction results from the collapse of one or more pharyngeal structures, such as the soft palate, the lateral pharyngeal walls, the tongue base, and/or the epiglottis[4–6].

DISE studies, which visualize epiglottic collapse (EC) better than traditional imaging techniques, have shown that epiglottic collapse occurs more often than previously described[6–8]. In fact, some studies have reported that up to 30% of patients have complete collapse of the epiglottis[7]. Research also indicates that epiglottic collapse is difficult to treat with conventional therapies, such as oral appliances[9] and even CPAP[10, 11]. Therefore, recognizing whether and how often a patient's upper airway collapses at the epiglottis could have important implications for treatment.

To determine whether epiglottic collapse contributes to OSA in a given patient, imaging techniques (e.g. computed tomography[12] and magnetic resonance imaging[13]) and DISE studies have been utilized. However, the invasive and expensive nature of these procedures hampers routine assessment of the structure causing collapse in the clinical setting. As an alternative approach, it has been shown that individuals with OSA exhibit well-defined, reproducible intra-breath airflow characteristics during sleep[14, 15]. Recently, our group has noted a link between one of these characteristics—the magnitude of negative effort dependence (NED, the reduction in airflow in association with increasing inspiratory effort—and the presence of epiglottic collapse in OSA[16]. Our results also suggested that rapid changes in inspiratory airflow within a breath ("discontinuities"), scored visually, were a recognizable hallmark of epiglottic collapse. However, to date, there has been no systematic investigation identifying epiglottic collapse from flow characteristics.

In this study, we hypothesized that epiglottic collapse has distinct and identifiable effects on the within-breath airflow shape during sleep in patients with OSA. We employed a machine learning approach to develop and validate a model that uses flow characteristics (features) to predict the presence versus absence of epiglottic collapse as defined by gold standard endoscopy. Endoscopy was performed simultaneously with flow measurement during natural sleep. As an additional clinical validation, pneumotachograph flow and nasal pressure were measured simultaneously on a separate subgroup of patients. The correlations between pneumotach- and nasal pressure-measured features were assessed.

METHODS

Participants

OSA patients (age: 21–70 years) with an apnea-hypopnea index (AHI) > 10 events/hr were invited to participate. The exclusion criteria included cardiac disease (uncontrolled hypertension or heart failure) or any other serious medical condition, and the use of medications known to influence sleep, respiration, or muscle control. The study was approved by the Partners Institutional Review Board. All participants provided written informed consent prior to study enrolment. The patients' characteristics and baseline PSG parameters were analyzed retrospectively.

Endoscopic studies

Measurements and Equipment—Participants were instrumented for a physiological polysomnographic study. Electroencephalography (EEG), chin electromyography (EMG), and electrooculography (EOG) were recorded for sleep staging. Piezo-electric bands around the chest and abdomen monitored respiratory movements/effort. Electrocardiography (ECG), body position, and arterial oxygen saturation (SaO2) were also recorded. In addition, participants wore a sealed nasal mask to facilitate airflow measurement using a pneumotach (Hans-Rudolph, Kansas City, MO). Mask pressure was monitored with a pressure transducer (Validyne, Northridge, CA) referenced to atmosphere. Pharyngeal lumen pressure was measured with a 5-french Millar catheter that had 6 pressure sensors 0.75 cm apart starting at the tip (P_1 to P_6 (downstream pressure sensor, placed above the epiglottis)). To visualize the airway, a 2.8 mm diameter pediatric bronchoscope was inserted through the second nostril. Spike 2 software (Cambridge Electronic Design, Cambridge, England) was used to acquire the physiological signals and endoscopic images. All signals except EEG, EMG, EOG, and ECG (which were sampled at 125 Hz) were captured at a sampling frequency of 500Hz, and the images were sampled at 30 frames/second.

Protocol—Participants were asked to sleep in either the supine or lateral position. To evaluate which pharyngeal structure was causing collapse, the scope's tip was initially placed above the soft palate and several flow-limited breaths were recorded. Flow limitation was determined based on simultaneous observations of flow and epiglottic pressure (lack of increase in flow despite decreasing epiglottic pressures). The tip of the scope was then advanced to the oropharynx to visualize the oropharyngeal and hypopharyngeal structures. This process was repeated with as many breaths being observed at both pharyngeal levels as possible throughout the night. While the scope was in the airway the whole night, videos were only recorded intermittently due to the technical limitations involved with handling the extremely large video files (e.g. limited memory on the local computer). In addition, breaths were excluded from the analysis if: 1) they occurred during wakefulness, REM sleep, or arousals, 2) they occurred during sleep in the lateral position because the occurrence of epiglottic collapse substantially decreases in this position[17], 3) they were not flow limited, or 4) secretions blurred the endoscopic view.

Breath Visualization and Gold Standard Classification—All eligible breaths were labeled as being associated with epigottic collapse or non-epiglottic collapse using the visual

inspection of the videos captured by the scope (in the velopharynx and oropharynx) during natural sleep. The breaths were labeled as epiglottic collapse if the epiglottis appeared to completely (or almost completely, >90% obstruction) close in either the anteroposterior or lateral direction (see online supplement for videos of both types of collapse and their associated flow patterns). In addition, to confirm that the flow limitation was not due to collapse of structure(s) above the epiglottis, the pressure just above the epiglottis was inspected and compared to mask pressure (the waveforms resemble one another when the epiglottis collapses, see Figure 2). This visual classification was performed by two investigators (MM and SO), with any discrepancies being resolved by a third investigator (AW).

Simultaneous Measurements of Pneumotachograph Flow and Nasal Pressure

For validation, pneumotach flow and nasal pressure were measured simultaneously (using an oronasal mask) in a separate subgroup of patients. A modified single-ended nasal cannula was used to measure nasal pressure. One end of nasal cannula was cut, sealed, and taped inside the mask and the other end was taped and passed through a sealed port in the mask and connected to a pressure transducer (Validyne, Northridge, CA). The nasal pressure (unfiltered, DC-coupled) was referenced to the mask pressure to measure the pressure difference between inside and outside the nostrils. To obtain a more accurate estimate of the pneumotach flow, the nasal pressure signal (PN) was linearized by different transformations, including, nasal pressure signal to the power of 0.75 ($\dot{V}_{PN}^{0.75}$, see online supplement for more details). To obtain the correlation coefficients between pneumotach and nasal pressure measured variables, breaths were randomly selected from this subgroup of patients.

Machine Learning and Algorithm Development

The algorithm development was performed independently by a separate investigator (AA) blinded to the visualization and gold standard classification process. For each breath, a total of 32 flow characteristics (features) were determined. The detailed calculations of these features are described in the online supplement. Briefly, the following important features were calculated: 1) Discontinuity index ($D1$), measured from the slope of the steepest line fitted to the inspiratory flow; 2) Inspiratory jaggedness index (JI_i) and expiratory jaggedness index (JI_e), which measure the extent of deviation from flatness in the inspiratory and expiratory flow (more variable flow results in a higher jaggedness index); 3) Respiratory parameters: the ratio of within-breath respiratory variables, such as the ratio of mean inspiratory flow and tidal volume ($\frac{\dot{V}mean}{VT}$), the ratio of the time of peak expiration and total expiration time ($\frac{Tmax_E}{T_e}$), and the ratio of peak expiratory flow and tidal volume ($\frac{\dot{V}max_E}{VT}$); 4) Fluttering index that quantifies the power of high frequency variations in the inspiratory flow normalized by squared tidal volume ($\frac{FP_i}{VT^2}$).

Classification

Here we use a classifier (i.e. equation or model) to define a boundary, based on flow characteristics, that best discriminates between breaths with versus without epiglottic

collapse. We employed an established approach to develop and validate a classifier (supervised learning[18]) whereby a model is trained based on gold standard classification (breath-by-breath endoscopic assessment), and tested in a set of data where the gold standard classification is hidden (10-fold cross validation). We used a "support vector machine classifier" which tends to outperform other types of classifiers[19–22]. See Figure 1 for an example implementation. In addition to the type of classifier, it is essential to select an optimal number of features to maximize the predictive value in the training and validation data sets. Adding more features may result in overfitting. To prevent overfitting, a sequential forward feature selection process[23] was performed within a 10-fold cross-validation[24] framework. Features were included in the model sequentially until there was no further improvement in predictive value based on the mean of *sensitivity* and *specificity* obtained from 10-fold cross-validation (i.e. N=7 features, see online supplement for a detailed description).

Statistical analyses

Data are expressed as the mean ± standard deviation (SD) or median (25^{th}–75^{th} percentile) unless otherwise specified. Unpaired two-tailed t-tests/Wilcoxon signed rank test were performed for between group comparisons. In addition to model development and validation, we also assessed whether breaths with epiglottic collapse were statistically associated with selected features using linear mixed model analysis[25, 26] (See online supplement for an example analysis). Statistical significance was accepted at $p<0.05$.

RESULTS

Patient characteristics

The endoscopy study involved twenty-three OSA patients (age: 49.9±9.3 years, 6 females) with an AHI of 48.6±30.4 events/hr and a body mass index of 32.8±6.0 kg/m^2. In addition, ten patients (age: 57.2±8.2 years, 2 females) with an AHI of 42.0±25.5 events/hr and a body mass index of 29.6±6.5 kg/m^2 were studied for simultaneous recording of pneumotach flow and nasal pressure. Tables 1 and 2 present the subjects' characteristics and PSG parameters.

Breaths verified by endoscopy

On average, 102±48 minutes of endoscopy video per subject in the supine position were obtained. A total of 1232 flow-limited breaths (54±61 breaths per subject) during supine NREM sleep were analyzed (after excluding breaths during wakefulness, arousals, excessive saliva, improperly-positioned scope, or otherwise poor visualization of the airway structures). From these breaths, using the visual inspection of endoscopy videos and pressure tracings, 244 (19.8%) were classified as epiglottic collapse, while 988 (80.2%) were classified as being associated with other sites of collapse.

Example traces

Figure 2 demonstrates example breaths that were associated with epiglottic collapse. The oropharyngeal view shows the epiglottis closing (or severely narrowing) at the beginning of inspiration, shown in Figure 2(a), resulting in an abrupt and severe reduction of airflow. This immediate reduction in airflow at the level of the epiglottis causes the upstream pressures

(e.g. P_5 and P_6) to become positive and follow the mask pressure. It also produces a discontinuity feature in the inspiratory flow that manifests as a fast rate of change in flow and a jagged inspiratory pattern. Figure 2(b) shows several example breaths that were associated with epiglottic collapse. A common feature is the presence of a discontinuity in the inspiratory flow. Breaths without epiglottic involvement, shown in Figure 3, clearly have different features, including fluttering and reduced "jaggedness". In addition, the "pressure dissociation" between P_3 and P_6, both of which are upstream to the epiglottis, suggest that the choke point is between these two sensors, i.e., at the level of the palate or tongue base.

Feature selection using 10-fold cross-validation

A total of 7/32 features were selected by our algorithm. The selected features were the discontinuity index ($D1$), inspiratory jaggedness index (JI_i), expiratory jaggedness index (JI_e), mean inspiratory flow normalized by tidal volume ($\frac{\dot{V}mean}{VT}$), relative time of expiratory peak ($\frac{Tmax_E}{T_e}$), inspiratory fluttering index ($\frac{FP_i}{VT^2}$), and peak expiratory flow normalized by tidal volume ($\frac{\dot{V}max_E}{VT}$). The final cross-validated accuracy ((*sensitivity* + *specificity*)/2) was 84% (validation data). The classification accuracy (training) was 87% (sensitivity = 96%, specificity=78%), indicating a loss of 3% in accuracy when tested on independent data.

Even though a nonlinear combination of these seven features (see online supplement) resulted in 84% cross-validated accuracy, the linear mixed model analysis revealed that epiglottic collapse was generally predicted by a higher discontinuity index ($D1$: 2.2 ± 0.38 points larger for breaths associated with epiglottic collapse, $p = 8.0\times10^{-9}$) and a higher inspiratory jaggedness index (JI_i: 0.09 ± 0.02 points larger for epiglottic-related breaths, $p = 1.1\times10^{-4}$). Figure 4 displays an example of the flow patterns associated with small and large values of these two features. Complementary results involving feature selection and linear mixed model analyses have been described in the online supplement.

Validation against nasal pressure recordings

A total of 1768 breaths (177±75 breaths per subject) were randomly selected from the polysomnography recordings that contained simultaneous measurements of pneumotach flow and nasal pressure (Figure 5). Discontinuity indices obtained from pneumotach flow were strongly associated with their concurrent values obtained from nasal pressure (Figure 6). The highest correlation was observed when flow was estimated by the nasal pressure to the power of 0.75 ($D1(\dot{V})$ Versus $D1(\dot{V}_{PN}{}^{0.75})$: r=0.8, p=0, Figure 6, see online supplement for correlation analysis involving different transformations). Similarly, there was a strong correlation between the inspiratory jaggedness index obtained from pneumotach flow and transformed nasal pressure ($JI_i(\dot{V})$ Versus $JI_i(\dot{V}_{PN}{}^{0.75})$: r=0.94, p=0, Figure 6). Other features resulted in similar correlations, indicating that epiglottic collapse can be reliably identified from nasal pressure recordings performed in clinical sleep laboratories.

DISCUSSION

The major conclusion of the current study is that epiglottic collapse produces flow features that: 1) are different from the features produced by non-epiglottic related obstructions, 2) are easy to quantify, and 3) can be reliably estimated from high fidelity (unfiltered, DC-coupled amplification) nasal pressure signals collected during clinical sleep studies. The main predictors of epiglottic collapse were discontinuity and jaggedness. Additional regression analysis of the simultaneously measured flow and nasal pressure features revealed identity relationships (linear relationship with slope≈1 and small intercept, correlation coefficients>0.8).

Prevalence and significance of epiglottic collapse

Previous studies have reported a wide variation in the prevalence of epiglottic collapse in OSA patients[6–8, 27]. This may be related to the inconsistent definition of epiglottic collapse in the literature. For instance, da Cunha Viana et al. reported that 42% of OSA patients had at least partial epiglottic collapse. However, when only obstructions with >75% narrowing were considered, epiglottic collapse was found in only 20% of the patients examined[27]. In our study, only complete or nearly complete obstruction of the epiglottis was considered as “epiglottic collapse.” The reasons for classifying it this way was three. First, we noticed that partial epiglottic collapse (e.g., 50–75% narrowing) virtually never produced a measurable reduction in flow (see Figure 2 and supplementary video). Second, “complete” collapse was easier to score and led to near perfect inter-rater agreement. Finally by restricting our definition to complete collapse, we felt more comfortable with categorizing the epiglottis as a dominant cause of obstruction. Previous studies have also argued that posterior movement of the tongue could cause the epiglottis to collapse[28]. However, this can be quite subjective and difficult to quantify endoscopically. Notably, in the many instances of epiglottic collapse examined in the current study, we often noticed the opposite, i.e., the tongue seemed to remain stationary or even move anteriorly slightly when the epiglottis collapsed. Future studies in which the tongue contribution to epiglottic collapse can be more systematically quantified are needed to explore this further.

Discontinuity and jaggedness as a signature of epiglottic collapse

The literature shows that OSA patients exhibit distinct and characteristic flow limitation patterns during sleep[14, 15]. Aittokallio et al found well-defined and reproducible flow shapes in different OSA patients. However, they did not try to correlate these shapes with anatomical structures within the airway. The results of the present study show that epiglottic collapse is associated with distinct flow shapes that can be quantified objectively. As described in our recent study, a cardinal feature of epiglottic collapse is the fact that it is intermittent[17]. In addition to its intermittency, this study shows that the most important feature distinguishing epiglottic collapse from other types of airway collapse is the presence of discontinuities in the flow (quantified by the discontinuity and jaggedness indices). Both of these features quantify the rapid decrease/increase in the airflow. Indeed, in the breaths examined in this study, the collapse of the epiglottis was observed to be severe and abrupt. In particular, anteroposterior movement of the epiglottis tended to be fast and unpredictable (see online supplementary video), occurring intermittently for unknown reasons. These

characteristic movements produced a sharp and severe reduction in airflow (Figure 2) that were captured by the discontinuity index proposed in this study. Also, the epiglottis was observed to be an unstable structure that would sometimes reopen/close repeatedly during inspiration causing a “jagged” flow (see Figure 2 and online video). These “unstable” movements were captured by both the discontinuity and jaggedness indices.

In addition to producing unique flow features, epiglottic collapse may also generate characteristic sounds that may be different than the non-epiglottic snoring sounds. Previous studies have reported a low prevalence of epiglottis related snoring among OSA patients[29, 30]. This, at least in our study, may be due to the fact that when the epiglottis collapses, particularly in the anteroposterior direction, the collapse is abrupt and thus the “classical” snoring sound may not be generated.

Discontinuity—This feature measures the slope of the steepest line fitted to the middle portion of the inspiratory airflow (after excluding trivial fast increases/decreases in flow at the start and end of inspiration). Figure 2 demonstrates a library of breaths with epiglottic collapse in which discontinuity (or very steep increases/decreases in flow) stands out as a signature of epiglottic collapse. The discontinuity index ($D1$), described in this study, reliably quantifies these fast flow variations. Additionally, detecting changepoints before measuring the slopes adds to the reliability of this measure by making it less sensitive to fast (low amplitude) fluctuations that are present when there is fluttering (Figure S1 (online supplement), Figure 3).

Jaggedness—The second important characteristic that is associated with epiglottic collapse is the presence of jaggedness in both inspiration and expiration. The jaggedness indices described in this study quantify the deviation of the airflow (inspiratory or expiratory) from a flat reference (mean airflow), as a result, the more variable the airflow around the mean, the higher the jaggedness index (Figure 4). This feature has been previously used by Teschler et al.[31] for automated CPAP-titration studies. In this study, we modified this feature by normalizing it to the inspiratory time to take into account the subject-specific differences in inspiratory time.

Reduced tidal volume—Selected features, including inspiratory fluttering index ($\frac{FP_i}{VT^2}$), $\frac{\dot{V}mean}{VT}$) and $\frac{\dot{V}max_E}{VT}$ were normalized by tidal volume and therefore are both a measure of the numerator and the tidal volume. A Wilcoxon signed rank test revealed that breaths associated with epiglottic collapse had lower tidal volume than non-epiglottic breaths (0.26±0.15 vs 0.31±0.15, $p < 0.0001$). In addition to quantifying the tidal volume, these features measure relative mean inspiratory flow, fluttering power (between 5Hz and 125Hz), and peak expiratory flow which resulted in an increase of 8% in cross-validated accuracy.

Validation against Nasal Pressure-Measured Flow

We used pneumotachograph-measured flow to develop the algorithm. However, since we hope this methodology will be adopted as a clinical tool, we validated it against high-fidelity nasal pressure signals (unfiltered, DC-coupled amplification) which can feasibly be assessed

clinically. The utility of nasal pressure airflow can be witnessed by the observed identity relationships (slope of linear fit≈1) and strong correlations between pneumotachograph-measured flow features and nasal pressure features (Figure 6). Of note, we used flow features that do not depend on absolute (calibrated) values of pneumotachograph-measured flow to facilitate implementation with uncalibrated flow signals.

Remaining Challenges for Clinical Use

The algorithm developed in this study automatically scores each breath as being associated with epiglottic or non-epiglottic collapse, yet ultimately these results require translation from “breath level” to a “patient level” for clinical decision making. Summarizing breath level data for an individual patient may be achieved by reporting the proportion of breaths with epiglottic collapse observed during sleep (per state, or per position), or the proportion of scored obstructive respiratory events (hypopneas) with epiglottic collapse. The optimal approach will be the one that best predicts responses to therapies.

Indeed, available evidence indicates that identifying the epiglottic collapse has important implications for OSA management[9, 32]. The method developed in this study can be used to test whether epiglottic collapse, assessed using this approach, predicts responses to therapy, including failure of oral appliances[9], surgery[33], increased occurrence of collapse on CPAP[10, 11, 32], and effectiveness of positional therapy[17, 32]. In addition, its utility as a screening tool for epiglottis-related surgery can be tested.

Limitations

This study has several limitations. First, due to the invasiveness of the study and the inherent challenges in performing endoscopy during natural sleep in OSA patients, our sample size was relatively modest (N=23). Nevertheless, the number of breaths (1232 breaths) examined was large enough that different flow patterns were equally well represented. Importantly, in the cross-validation framework, the number of features (7 features) was far less than the number of observations (123 in each fold) which made the training procedure more robust. Furthermore, 10 fold cross-validation was also used to prevent overfitting that occurs when the sample size is small. Second, the number of breaths analyzed was different among subjects which could potentially bias the algorithm towards patients with more breaths. However, this was dealt with in two ways. First, the 10-fold cross validation framework allows for the “rare cases” to be left out of the analysis and be tested with the model built with the majority cases. If the model was biased towards the majority cases, it would result in a lower overall accuracy. In this study, a 3% difference was observed between classification accuracy (when the model was built and tested using the whole data set) and cross validation accuracy (when the model was built using 90% of the data and was tested on the remaining 10%) which suggests that if the algorithm were to be tested on a new data set, the potential loss of accuracy would be around 3%. Secondly, linear mixed effect models for selected features show that three out of 7 selected features are significantly different between the two groups.

A third limitation relates to the storage of large video files during endoscopy. For every minute of recording, the system produced approximately 1.1 GB of data, which limited our

ability to store the video files continuously throughout the night. Nevertheless, we recorded an average of 148±49 minutes of endoscopic images per subject from the first and second halves of the night to have a well-represented library of different sites of collapse/flow patterns. Also, the video files were stored in small files every 5–10 minutes to prevent missing frames and desynchronization between the signals and videos. The final limitation is that the presence of inspiratory flow is required for the algorithm to function properly. Therefore, the method presented here would not identify epiglottic collapse from a patient whose respiratory events were mostly apneas.

Conclusions

In this study, an automated algorithm was developed to objectively identify breaths with epiglottic collapse as distinct from other sites of collapse. We demonstrate that an epiglottic contribution to OSA is characterized by the presence of “discontinuity” and “jaggedness”. Since the presence of epiglottic collapse seen using endoscopy has implications for success versus failure of OSA therapies[9–11, 32, 33], we envisage that our algorithm will enable rapid, non-invasive identification of epiglottic involvement without requiring invasive endoscopy.

Supplementary Material

Refer to Web version on PubMed Central for supplementary material.

Acknowledgments

This work was performed at the Brigham and Women’s Hospital and Harvard Medical School and was supported by funding from Fan Hongbing, President of OMPA Corporation, Kaifeng, China, Philips Respironics research grant, the National Institutes of Health grants (R01 HL 128658, 2R01HL102321 and P01 NIH HL095491), as well as the Harvard Catalyst Clinical Research Center (UL1 RR 025758-01). Dr. Sands was supported by the National Health and Medical Research Council of Australia (1053201), Menzies Foundation, the American Heart Association (15SDG25890059), and American Thoracic Society Foundation. Dr. Taranto-Montemurro is supported by the American Heart Association (17POST33410436). Dr. Marques was supported by FAPESP.

References

1. Young T, Peppard P, Gottlieb D. The epidemiology of obstructive sleep apnea: a population health perspective. Am J Respir Crit Care Med. 2002; 165:1217–1239. [PubMed: 11991871]
2. Colt HG, Hass H, Rich GB. Hypoxemia vs sleep fragmentation as cause of excessive daytime sleepiness in obstructive sleep apnea. CHEST Journal. 1991; 100(6):1542–1548.
3. Davies CWH, Crosby JH, Mullins RL, Barbour C, Davies RJ, Sradling JR. Case-control study of 24 hour ambulatory blood pressure in patients with obstructive sleep apnoea and normal matched control subjects. Thorax. 2000; 55(9):736–740. [PubMed: 10950890]
4. Kezirian EJ, Hohenhorst W, de Vries N. Drug-induced sleep endoscopy: the VOTE classification. Eur Arch Otorhinolaryngol. 2011; 268(8):1233–1236. [PubMed: 21614467]
5. Vroegop AV, Vanderveken OM, Boudewyns AN, Scholman J, Saldien V, Wouters K, Braem MJ, Van de Heyning PH, Hamans E. Drug-induced sleep endoscopy in sleep-disordered breathing: report on 1,249 cases. Laryngoscope. 2014; 124(3):797–802. [PubMed: 24155050]
6. Ravesloot MJ, Vries Nd. One hundred consecutive patients undergoing drug-induced sleep endoscopy: results and evaluation. Laryngoscope. 2011; 121(12):2710–2716. [PubMed: 22109770]
7. Lan MC, Liu SY, Lan MY, Modi R, Capasso R. Lateral pharyngeal wall collapse associated with hypoxemia in obstructive sleep apnea. Laryngoscope. 2015; 125(10):2408–2412. [PubMed: 25582498]

8. Cavaliere M, Russo F, Iemma M. Awake versus drug-induced sleep endoscopy: evaluation of airway obstruction in obstructive sleep apnea/hypopnoea syndrome. Laryngoscope. 2013; 123(9):2315–2318. [PubMed: 24167821]

9. Kent DT, Rogers R, Soose RJ. Drug-Induced Sedation Endoscopy in the Evaluation of OSA Patients with Incomplete Oral Appliance Therapy Response. Otolaryngol Head Neck Surg. 2015; 153(2): 302–307. [PubMed: 26044788]

10. Verse T, Pirsig W. Age-related changes in the epiglottis causing failure of nasal continuous positive airway pressure therapy. J Laryngol Otol. 1999; 113(11):1022–1025. [PubMed: 10696386]

11. Shimohata T, Shinoda H, Nakayama H, Ozawa T, Terajima K, Yoshizawa H, Matsuzawa Y, Onodera O, Naruse S, Tanaka K, Takahashi S, Gejyo F, Nishizawa M. Daytime hypoxemia, sleep-disordered breathing, and laryngopharyngeal findings in multiple system atrophy. Arch Neurol. 2007; 64(6):856–861. [PubMed: 17562934]

12. Yucel A, Unlu M, Haktanir A, Acar M, Fidan F. Evaluation of the upper airway cross-sectional area changes in different degrees of severity of obstructive sleep apnea syndrome: cephalometric and dynamic CT study. AJNR Am J Neuroradiol. 2005; 26(10):2624–2629. [PubMed: 16286412]

13. Huon LK, Liu SY, Shih TT, Chen YJ, Lo MT, Wang PC. Dynamic upper airway collapse observed from sleep MRI: BMI-matched severe and mild OSA patients. Eur Arch Otorhinolaryngol. 2016; 273(11):4021–4026. [PubMed: 27276991]

14. Aittokallio T, Gyllenberg M, Saaresranta T, Polo O. Prediction of inspiratory flow shapes during sleep with a mathematic model of upper airway forces. Sleep. 2003; 26(7):857–863. (Journal Article). [PubMed: 14655920]

15. Aittokallio T, Saaresranta T, Polo-Kantola P, Nevalainen O, Polo O. Analysis of inspiratory flow shapes in patients with partial upper-airway obstruction during sleep. Chest. 2001; 119(1):37–44. [PubMed: 11157582]

16. Genta PR, Edwards BA, Sands SA, Owens R, Butler JP, Loring SH, Kezirian EJ, Demko BG, Kats ES, White DP, Wellman A. Identifying the Upper Airway Structure Causing Collapse in Obstructive Sleep Apnea by the Shape of Airflow. American Thoracic Society. May 1.2015 :A5604.

17. Marques MO, Genta PR, Sands SA, Azarbarzin A, de Melo C, Taranto-Montemurro L, White DP, Wellman A. Effect of sleeping position on upper airway patency in obstructive sleep apnea is determined by the pharyngeal structure causing collapse. Sleep. 2017 In Press.

18. Moller M. Supervised learning on large redundant training sets. Int J Neural Syst. 1993; 4(1):15–25. [PubMed: 8049786]

19. Huang HH, Xu T, Yang J. Comparing logistic regression, support vector machines, and permanental classification methods in predicting hypertension. BMC Proc. 2014; 8(Suppl 1):S96. [PubMed: 25519351]

20. McQuisten KA, Peek AS. Comparing artificial neural networks, general linear models and support vector machines in building predictive models for small interfering RNAs. PLoS ONE. 2009; 4(10):e7522. [PubMed: 19847297]

21. Judson R, Elloumi F, Setzer RW, Li Z, Shah I. A comparison of machine learning algorithms for chemical toxicity classification using a simulated multi-scale data model. BMC Bioinformatics. 2008; 9:241. [PubMed: 18489778]

22. Fernandez-Delgado M, Cernadas E, Barro S. Do we Need Hundreds of Classifiers to Solve Real World Classification Problems? Journal of Machine Learning Research. 2014; 15:3133–3181.

23. Guyon I, Elisseeff A. An introduction to variable and feature selection. JMachLearnRes. 2003; 3:1157–1182. Journal Article.

24. Kohavi, R. A study of cross-validation and bootstrap for accuracy estimation and model selection. Int Joint Conf on Artificial Intelligence (IJCAI); 1995; Montreal, Canada. p. 1137-1143.

25. Winter, B. Linear models and linear mixed effects models in R with linguistic applications. arXiv. 2013. 1308.5499 [http://arxiv.org/pdf/1308.5499.pdf]

26. Baayen RH, Davidson DJ, Bates DM. Mixed-effects modeling with crossed random effects for subjects and items. Journal of Memory and Language. 2008; 59:390–412.

27. da Cunha Viana A Jr, Mendes DL, de Andrade Lemes LN, Thuler LC, Neves DD, de Araujo-Melo MH. Drug-induced sleep endoscopy in the obstructive sleep apnea: comparison between NOHL

and VOTE classifications. Eur Arch Otorhinolaryngol. 2017; 274(2):627–635. [PubMed: 27164944]

28. Lin HS, Rowley JA, Badr MS, Folbe AJ, Yoo GH, Victor L, Mathog RH, Chen W. Transoral robotic surgery for treatment of obstructive sleep apnea-hypopnea syndrome. Laryngoscope. 2013; 123(7):1811–1816. [PubMed: 23553290]
29. Quinn SJ, Huang L, Ellis PD, Williams JE. The differentiation of snoring mechanisms using sound analysis. Clin Otolaryngol Allied Sci. 1996; 21(2):119–123. [PubMed: 8735394]
30. Saunders NA, Vandeleur T, Deves J, Salmon A, Gyulay S, Crocker B, Hensley M. Uvulopalatopharyngoplasty as a treatment for snoring. Med J Aust. 1989; 150(4):177–182. [PubMed: 2716600]
31. Teschler H, Berthon-Jones M, Thompson AB, Henkel A, Henry J, Konietzko N. Automated Continuous Positive Airway Pressure Titration for Obstructive Sleep Apnea Syndrome. Am J Respir Crit Care Med. 1996; 154:734–740. [PubMed: 8810613]
32. Torre C, Camacho M, Liu SY, Huon LK, Capasso R. Epiglottis collapse in adult obstructive sleep apnea: A systematic review. Laryngoscope. 2016; 126(2):515–523. [PubMed: 26371602]
33. Kezirian EJ. Nonresponders to pharyngeal surgery for obstructive sleep apnea: insights from drug-induced sleep endoscopy. Laryngoscope. 2011; 121(6):1320–1326. [PubMed: 21557231]

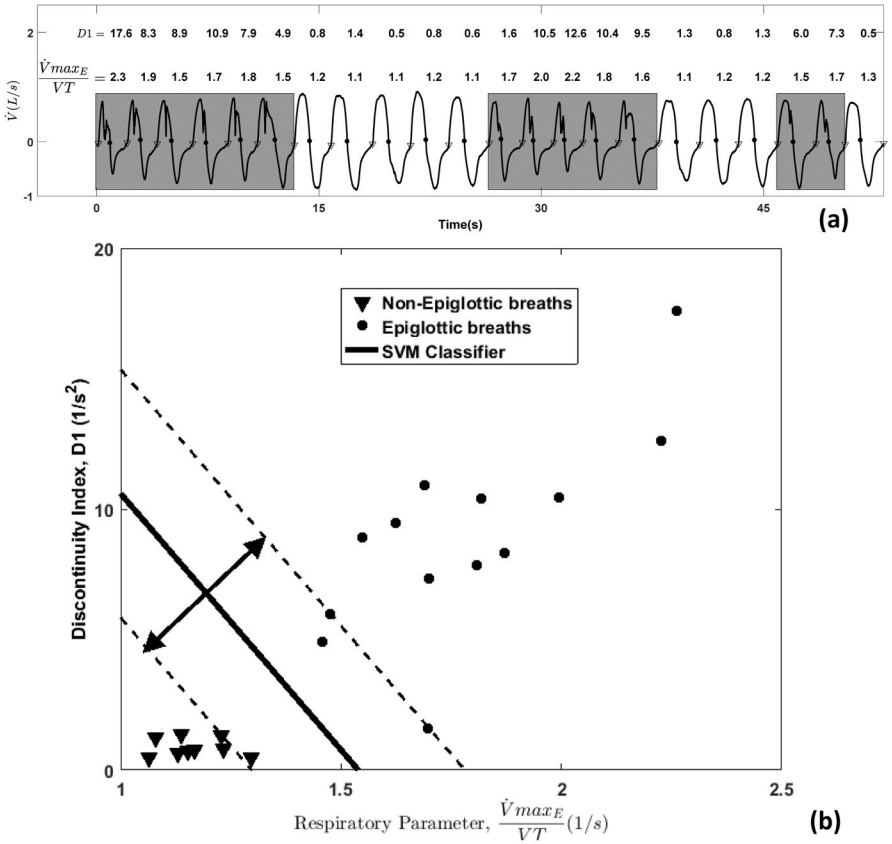

Figure 1.

In this simplified example classification scheme (support vector machine), we take 22 breaths, 13 of which have epiglottic collapse. a) Two characteristics (features) are highlighted, the discontinuity index (D1) and respiratory parameter ($\frac{\dot{V}\text{max}_E}{VT}$: the ratio of peak expiratory flow and tidal volume), and overlaid on the flow trace. b) Plot of characteristics for breaths with epiglottic collapse (circles) versus without epiglottic collapse (triangles). The classifier finds a linear boundary between groups that maximizes the margin of error (arrows, dashed lines).

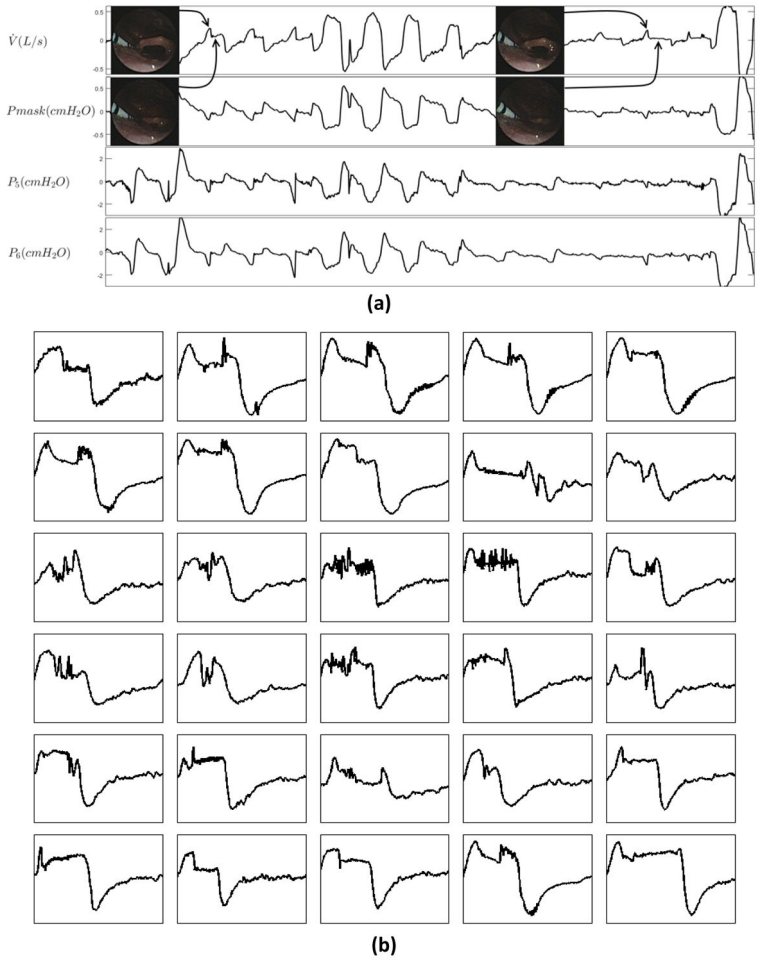

Figure 2.

(a) Epiglottic collapse accompanied by distinct flow characteristics (e.g. discontinuities in inspiratory flow). The pressure above the epiglottis (P_5 and P_6, downstream to P_5) closely follows the mask pressure, confirming that the airway above the epiglottis is patent. (b) Examples of epiglottic collapse associated with sudden flow change.

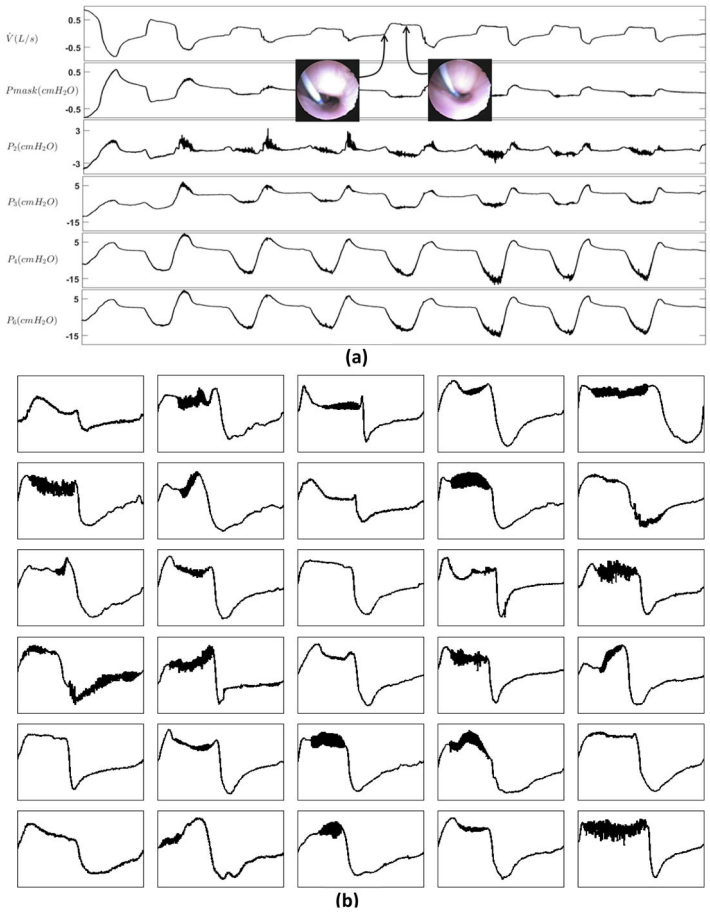

Figure 3.

Non-epiglottic pharyngeal collapse often produces a “flat-top” flow shape. (a) The multi-tip pressure tracings suggest that there is a choke point between P_3 and P_4. (b) Example traces of non-Epiglottic collapse.

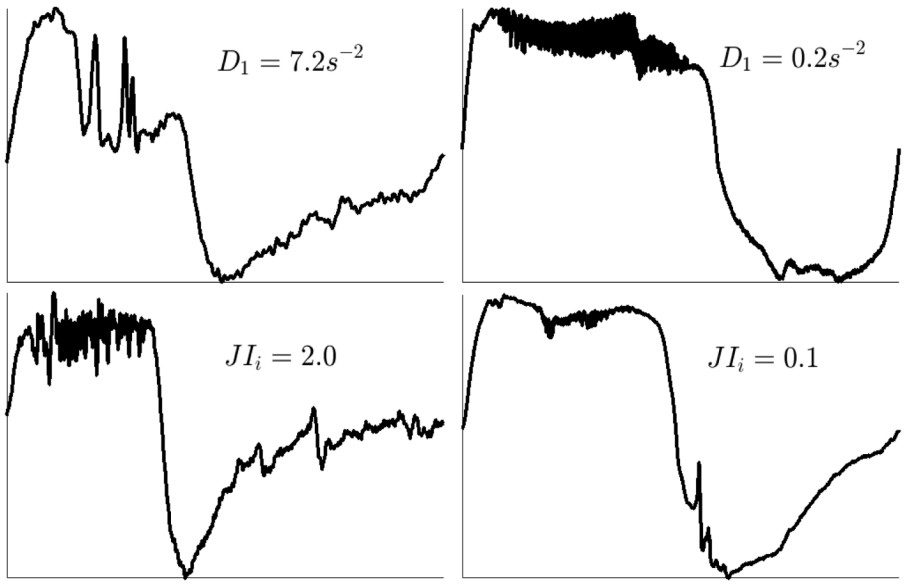

Figure 4.

Large value of the discontinuity index (D1) and the inspiratory jaggedness index (JI_i) predict epiglottic collapse. The left column displays the flow patterns associated with high values of the discontinuity index and jaggedness index whereas the right column represents the flow patterns associated with low values of these features.

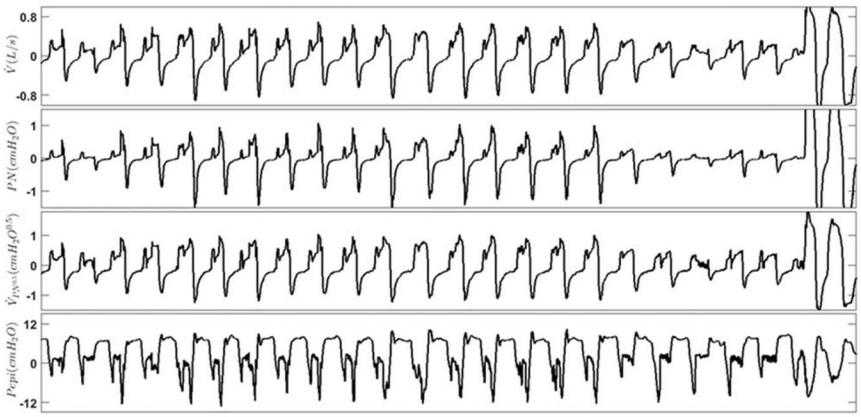

Figure 5.

The discontinuity and jaggedness features associated with epiglottis collapse were reliably captured by nasal cannula. These features were preserved in these example breaths that were simultaneously collected using pneumotachograph (first (top) panel, $\dot{V}$) and a nasal cannula (second panel, PN). To estimate the pneumotach flow, the nasal pressure signal was passed through a square root transformation (third panel, $\dot{V}_{PN}{}^{0.5}$). The bottom panel shows the pressure above the epiglottis (Pepi), indicating epiglottic collapse.

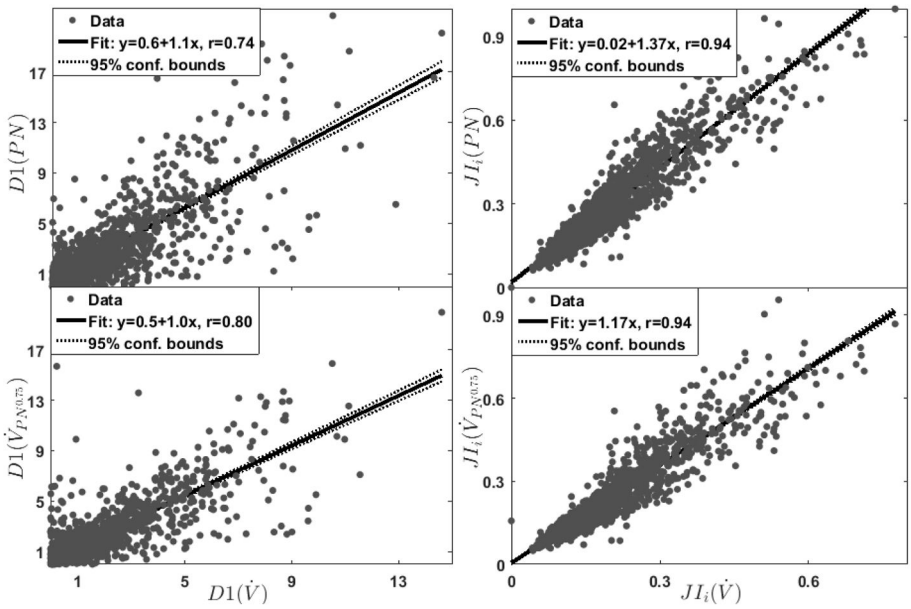

Figure 6.

The discontinuity and jaggedness features obtained from pneumotachograph measured flow ($\dot{V}$) were strongly correlated with their corresponding values obtained from nasal pressure (PN). A stronger correlation was obtained when nasal pressure was transformed ($\dot{V}_{PN}^{0.5}$, bottom row) compared with untransformed nasal pressure (PN, top row).

Table 1

Participants' anthropometric parameters

	Endoscopy Physiology Study (N=23)				Nasal Pressure Study (N=10)
	All subjects (n=23)	**Non-epiglottic collapse (n=18)**	**Epiglottic collapse (n=5)**	**p**	
Age (years)	49.9 ± 9.3	47.8 ± 8.7	57.4 ± 7.6	0.038	57.2 ± 8.2
Sex (M:F)	17:6	12:6	5:0	0.3[a]	8:2
Neck circumference (cm)	40.7 ± 4.5	40.7 ± 4.9[b]	40.8 ± 3.4	>0.9	41.5 ± 3.4
BMI (kg/m^2)	32.8 ± 6.0	33.0 ± 5.8	32.1 ± 7.2	0.8	29.6 ± 6.5
Mallampati Score	3.5 ± 0.7	3.6 ± 0.6[c]	3.3 ± 1.0[c]	0.4	—
Total endoscopy recording (min)	149.8 ± 49.3	143.4 ± 54.2	166.2 ± 19.4	0.4	—

Data are presented as mean ± standard deviation. BMI: body mass index;

[a] Evaluated by Fisher's exact test.

[b] one data point is missing from the group.

[c] Two data points are missing from calculation.

Table 2

Participants' polysomnographic parameters

	Endoscopy Physiology Study (N=23)*				Nasal Pressure Study (N=10)
	All subjects (n=23)	**Non-epiglottic collapse (n=18)**	**Epiglottic collapse (n=5)**	**p**	
TST(min)	291 ± 93 [a]	286 ± 99 [a]	305 ± 76 [a]	0.7	306 ± 70.9
SE (%)	70.4 ± 14.4 [a]	71.0 ± 14.6 [a]	68.5 ± 15.0 [a]	0.7	71.9 ± 13.9
NREM 1(%TST)	27.6 ± 24.8 [a]	27.0 ± 26.4 [a]	29.4 ± 22.1 [a]	0.9	28.2 ± 20.1
NREM 2(%TST)	57.0 ± 20.2 [a]	56.8 ± 21.3 [a]	57.6 ± 18.5 [a]	>0.9	56.2 ± 16.3
NREM 3(%TST)	1.5 ± 2.9 [a]	1.6 ± 3.1 [a]	1.0 ± 2.3 [a]	0.7	6.8 ± 13.9
REM(%TST)	14.1 ± 8.9 [a]	14.8 ± 8.5 [a c]	12.1 ± 10.6 [a]	0.6	8.8 ± 6.0
AHI (events/hour)	48.6 ± 30.4	51.1 ± 33.0	40.7 ± 20.8	0.5	42.0 ± 25.5
ArI (events/hour)	43.0 ± 31.3 [a]	42.3 ± 34.6 [a]	45.3 ± 20.3 [a]	0.9	44.7 ± 20.1
Nadir SaO_2 (%)	81.7 ± 9.4 [a]	83.1 ± 8.4 [a]	77.2 ± 12.0 [a]	0.2	83.4 ± 12.5

Data are presented as mean ± standard deviation.

*Polysomnography data were analyzed retrospectively.

TST: total sleep time; SE: sleep efficiency; NREM 1, NREM 2, NREM 3: non-rapid eye movement sleep stages 1–3; AHI: apnea-hypopnea index; ArI: arousal index; SaO_2: oxygen hemoglobinic saturation.

[a]Two data points are missing from calculation.